



Published in final edited form as:

Transl Stroke Res. 2020 February ; 11(1): 108–121. doi:10.1007/s12975-019-00694-y.

Functional dynamics of neutrophils after ischemic stroke

Wei Cai, MD, PhD^{1,2,*}, Sanxin Liu, MD^{1,*}, Mengyan Hu, MD^{1,*}, Feng Huang, MD², Qiang Zhu, MD¹, Wei Qiu, MD, PhD¹, Xiaoming Hu, MD, PhD³, Jacob Colello⁴, Song Guo Zheng, MD, PhD^{4,#}, Zhengqi Lu, MD, PhD^{1,#}

¹Department of Neurology, the Third Affiliated Hospital of Sun Yat-sen University, People's Republic of China

²Center of Clinical Immunology, the Third Affiliated Hospital of Sun Yat-sen University, People's Republic of China

³Pittsburgh Institute of Brain Disorders and Recovery, and Department of Neurology, University of Pittsburgh School of Medicine, Pittsburgh, PA 15213, USA

⁴Department of Internal Medicine, Ohio State University College of Medicine and Wexner Medical Center, Columbus, OH 43201, USA

Abstract

Neutrophils are forerunners to brain lesions after ischemic stroke and exert elaborate functions. However, temporal alterations of cell count, polarity, extra cellular trap formation and clearance of neutrophils remain poorly understood. The current study was aimed at providing basic information of neutrophil functional throughout a time course following stroke with patients and animal study. We found that neutrophil constitution in peripheral blood increased soon after stroke onset of patients, and higher neutrophil count indicated detrimental stroke outcomes. Comparably, neutrophil count in peripheral blood of stroke mice peaked at the 12h after cerebral ischemia, followed by a 1-2d spike in brain lesions. In stroke lesion, clearance of neutrophils peaked at 2d after stroke and extracellular traps were mostly detected at 2-3d after stroke. In neutrophil

#Corresponding author: Dr. Zhengqi Lu, Department of Neurology, The third affiliated hospital of Sun Yat-sen University, 600 Tianhe Road, Guangzhou, Guangdong 510630, China, Tel: 020-85253203; Fax: 020-85253262; lzq1828@outlook.com; Dr. Song Guo Zheng, Department of Internal Medicine, Ohio State University Ohio State University, College of Medicine and Wexner Medical Center, Columbus, OH 43201, USA, Tel: 614 293 7452; Fax: 614 266 0980; SongGuo.Zheng@osumc.edu.

Authors' contributions

W.C. designed and performed the experiments, collected and analyzed data, and drafted the manuscript. S.L. carried out immunostaining, imaging and quantification, and drafted the manuscript. M.H. performed animal experiments and collected data. F.H. and Q.Z. contributed to the experimental design and the manuscript. W.Q. designed the experiment and critically revised the manuscript. X.H. contributed to the experimental design and revised the manuscript. S.G.Z and Z.L. designed and supervised the study and critically revised the manuscript. J.C. edited and revised MS. All authors read and approved the final manuscript.

*Wei Cai, Sanxin Liu and Mengyan Hu contribute equally to this project.

Conflict of Interest

The authors declare no conflicts of interest.

Ethics approval

All animal experiments were approved by the Third Affiliated Hospital of Sun Yat-sen University and performed following the Guide for the Care and Use of Laboratory Animals and Stroke Treatment. Clinic research was approved by the ethics committee of the Third Affiliated Hospital of Sun Yat-sen University.

Consent for publication

Not applicable.

Availability of data and materials

The datasets used and/or analyzed during the current study are available from the corresponding author on reasonable request.

infiltrated into stroke lesion, expression of the N2 marker CD206 was relatively stable. We found that N2 phenotype facilitated neutrophil clearance by macrophage and did not further induce neuronal death after ischemic injury compared with N0 or N1 neutrophils. Skewing neutrophil towards N2 phenotype before stroke reduced infarct volumes at 1d after tMCAO. Conditioned medium of ischemic neurons drove neutrophils away from the protective N2 phenotype and increased formation of extracellular traps. Conclusively, neutrophil function has an important impact on stroke outcomes. Neutrophil frequency in the peripheral blood could be an early indicator of stroke outcomes. N2 neutrophils facilitate macrophage phagocytosis and are less harmful to ischemic neurons. Directing neutrophils towards N2 phenotype could be a promising therapeutic approach for ischemic stroke.

Keywords

brain ischemia; neutrophils; extracellular traps; neuroprotection

Introduction

Cerebral ischemic stroke is a multi-phasic disorder [1,2]. Following the primary ischemic injury, inflammatory responses cause secondary exacerbation to the lesion. Neutrophils are among the forerunners to the ischemic brain after cerebral ischemia [3,4]. Once summoned by neutrophil attracting chemokines [5] to the stroke lesion, neutrophils display functional heterogeneity. Polarization of neutrophils towards the N2 phenotype has been demonstrated to be protective in ischemic stroke [6]. After executing their function, neutrophils are cleared by microglia/macrophages, which is facilitated by N2 polarization [6]. Neutrophil extracellular traps (NETs) were considered a programmed cell death mechanism to combat invading microorganisms [7]. It is not until recently that NETs were detected in aseptic inflammatory lesions [8]. To date, no evidence of NETs formation in ischemic brain or its influence to injured neurons has been documented.

Neutrophils exert elaborate functions in the ischemic brain. Nevertheless, the time course of the aforementioned processes has not been fully explored. The aim of the current study was to depict the functional dynamics of neutrophils after ischemic stroke, including time course of neutrophil infiltration, polarization and clearance by microglia/macrophages. NETs formation after ischemic stroke was analyzed. Interaction between ischemic neuron and neutrophil was also explored.

Materials and method

Patients

The current research was approved by the ethics committee of the Third Affiliated Hospital of Sun Yat-sen University. Clinic files of 294 consecutive Chinese patients (ethnic Han) with acute ischemic stroke (AIS) admitted within 24h of symptom onset in the Third Affiliated Hospital from January 1st, 2014 to August 10th, 2018 were reviewed. Among them, 17 patients were diagnosed as secondary ischemic stroke, 11 patients with malignant tumor, and 9 patients with cerebral hemorrhagic transformation. Additionally, 32 patients who had no

MRI data were excluded. Altogether, 225 patients were included in the study, 58 of which had infection (including respiratory infection and urinary infection) and 167 without. Among those with infection, 34 patients had infarction > 1.5cm and 24 had infarction 1.5cm [9-11]. In patients without infection, 74 of them had infarction > 1.5cm and 93 of them had infarction 1.5cm. The inclusion process was shown in Fig. S1. Age (mean 64.87 ± 0.60 and 95% CI 63.69 – 66.05), gender (female : male = 68 : 157), and score of National Institute stroke scale [12,13] (NIHSS) of patients were recorded. Neutrophil count, neutrophil to lymphocyte ratio (NLR) in the peripheral blood and the infarct sizes within 24h after symptom onset were analyzed. A total of 56 age and gender matched healthy controls (HC) were included in the study. Patient demographics including co-morbidities were summarized in Table S1.

Animals

C57BL/6 wild type mice (8- to 12-week-old, weight 18-25g) were purchased from Guangdong Medical Laboratory Animal Center (Guangzhou, China), and housed in a humidity- and temperature-controlled animal facility in Sun Yat-sen University with a 12-hour light-dark cycle for at least 1 week before induction of ischemic stroke. Food and water were freely accessible. All the experimental protocols were approved by the Animal Care and Use Committee of Sun Yat-sen University following the Guide for the Care and Use of Laboratory Animals. A total of 152 male mice were used in transient middle cerebral artery occlusion (tMCAO) model, including 20 mice that were excluded from further assessments due to death after ischemia or unsuccessful induction of stroke. The mortality rate was 0% in 1h and 3h stroke mice, 10% in 6h stroke mice, 18.18% in 12h stroke mice, 25% in 1d stroke mice, 25% in 2d stroke mice, 25% in 3d stroke mice, 33.33% in 5d stroke mice, 42.86% in 7d stroke mice, and 0% in sham animals. There were 30 male mice used for primary neutrophil- or macrophage-enriched culture, and 6 pregnant mice used for primary cortical neuronal culture.

Experiment protocol

Experiment 1—Neutrophil alteration in patients with acute ischemic stroke and its correlation with stroke outcomes was evaluated. Neutrophil counts and NLR in the peripheral blood of patients and healthy control (HC) were assessed. NIHSS scores and infarct sizes of patient on admission were analyzed. Correlation analysis of NIHSS scores/ infarct sizes with neutrophil counts/NLR was conducted.

Experiment 2—Numbers of neutrophil in infarct brain and peripheral blood could be influenced with infection, and infection commonly occurs after stroke due to immune compromise. As to better exclude the impact of infection on neutrophil fluctuation and testify the correlation between neutrophil elevation and infarct sizes, mice were pretreated with board spectrum antibiotics to prevent infection. Cerebral ischemia was then induced and correlation analysis between neutrophil frequency in blood and infarct volumes of mice was performed. Internal comparison of the cohort was conducted with all animals pretreated with antibiotics.

Experiment 3—So as to investigate temporal, spatial and functional dynamics of neutrophils after stroke, cerebral ischemia was induced in mice and samples were collected at various time points. Neutrophil percentages in bone marrow, peripheral blood and spleen, infiltration pattern in ischemic brain lesion, phenotypic shift, extracellular trap formation and withdrawal time line were assessed with flow cytometry at 6h, 12h, 1d, 2d, 3d, 5d and 7d after stroke. Expression of neutrophil attracting chemokines and neutrophil functional factors in ipsilateral brain were evaluated with real time polymerase chain reaction (RT-PCR) at 1h, 3h, 6h, 12h, 24h and 48h after cerebral ischemia. To visualize NETs in stroke lesion, immuno-staining of citrullinated histone H3 (CitH3) or Sytox green and neutrophil elastase (NE) in brain slices, and scanning electronic microscopy (SEM) experiments were performed.

Experiment 4—In order to evaluate the impact of neutrophil polarity and NETs formation on phagocytosis in macrophages, N0, N1, N2 and NETs forming neutrophils were prepared and subjected to macrophages for phagocytosis. The numbers of neutrophils engulfed by macrophages were calculated.

Experiment 5—As to investigate the impact of neutrophil polarity to stroke outcomes, neutrophil was skewed to N2 phenotype with transforming growth factor beta (TGFβ). Comparison of infarct volumes between the TGFβ treated mice with PBS treated controls was conducted.

Experiment 6—To evaluate the interaction between neutrophils and ischemic neurons, *in vitro* experiments were performed. Primary cultured mice neurons were subjected to oxygen glucose deprivation (OGD), followed by co-culturing with various phenotypes of neutrophils or treatment with neutrophil conditioned medium (CM). Viability of the ischemic neurons after a 24h treatment was assessed with immuno-staining of neuronal nuclei (NeuN). Furthermore, conditioned medium of post-OGD neurons was collected and treated with N0 neutrophils. Neutrophil polarization and NETs formation after treatment were analyzed.

MRI Scanning and Infarct Volume Analysis of Patients

Magnetic resonance imaging (MRI) was performed within 24h of admission using 1.5- or 3.0-T magnetic resonance imaging (Signa; GE Medical Systems, Milwaukee, WI, USA). In this study, the diffusion-weighted imaging (DWI) spin-echo planar sequence included 20 contiguous axial oblique slices ($b = 0$ and 1000s/mm^2 iso-tropically weighted; repetition time/echo time, 6000/60.4ms; acquisition matrix, 128×128 ; slice thickness, 5mm; interslice gap, 1mm; field of view, 24cm). DWI lesions in 225 patients were measured with Analyze 7.0 software (Analyze Direct, KS). Cerebral infarct sizes were assessed by largest infarct diameter determined on the image demonstrating the largest lesion [14]. MRI scans of patients were assessed by experienced neurologists Zhengqi Lu and Sanxin Liu, who were blinded to the patients' clinical features. All images were interpreted with the same window settings, same types of monitors and lighting conditions.

Murine Model of Transient Focal Ischemia

Focal ischemic stroke model was induced in mice with transient middle cerebral artery occlusion (tMCAO) as described previously [15]. Briefly, mice were anesthetized with 1.5% isoflurane in air under spontaneous breathing. A midline neck incision was made and soft tissues over the trachea were retracted gently. The left common carotid artery (CCA) was isolated and ligated temporarily. A permanent knot was placed on the distal part of external carotid artery (ECA) and a loose temporal knot was placed on both the proximal part of ECA. A tight temporal knot was placed on the internal carotid artery (ICA). ECA was cut between the permanent knot and the temporal knot, a filament was inserted into ECA and directed to middle cerebral artery (MCA) through ICA after loosening the temporal knot on ICA. Once the filament insertion into the MCA was confirmed, the loose temporal knot on ECA was tightened and the temporal knot on CCA was loosened. Filament insertion into the ICA was maintained for 60min followed by reperfusion. Sham-operated animals underwent the same anesthesia and surgical procedures but were not subjected to arterial occlusion. Core body temperatures were maintained with a heating pad. Regional cerebral blood flow (rCBF) during the surgery was measured by laser Doppler flowmetry. Mice with less than 70% reduction of blood flow in the ischemic core or those died during surgery were excluded from further analysis. As to skew neutrophil polarization towards N2 phenotype, TGF β (2ug per mouse) was i.v. injected to animals at 1d before tMCAO. Blood samples were collected at 1d after TGF β injection right before tMCAO surgery and neutrophil polarity was assessed.

Immunofluorescence Staining and Quantification

Mice were sacrificed at 6h, 12h, 1d, 2d, 3d and 5d after tMCAO and perfused with saline followed by PBS containing 4% paraformaldehyde (PFA, Sigma-Aldrich). Brains were removed and cut into 25- μ m frozen cryosections using a microtome. Brain sections were incubated with primary antibodies at 4°C overnight. After wash in PBS, sections were incubated with secondary antibodies for 1 hour at room temperature. Sections were then washed and mounted with DAPI Fluoromount-G (Southern Biotech). The following primary antibodies were used: rat anti-Ly6G (1:500, BD bioscience), goat anti-Iba1 (1:500, Abcam), goat anti-CD206 (1:500, R&D system), rabbit anti-CitH3 (1:500, Abcam), and rabbit anti-MPO (1:500, R&D system). The following secondary antibodies were applied: anti-rabbit secondary antibody conjugated with Cy3 (1:1000, Jackson ImmunoResearch Laboratories), anti-rabbit secondary antibody conjugated with Alexa Fluor 488 (1:1000, Jackson ImmunoResearch Laboratories), anti-rat secondary antibody conjugated with Alexa Fluor 488 (1:1000, Jackson ImmunoResearch Laboratories), anti-goat secondary antibody conjugated with Alexa Fluor 488 (1:1000, Jackson ImmunoResearch Laboratories). For detection of formation of neutrophil extra cellular traps (NETs), brain sections from mice sacrificed at 2d after tMCAO were stained with chromatin dye Sytox green (Invitrogen, 5mM in HBSS) and neutrophil elastase (NE, 1:200 abcam). To assess neuronal viability, neurons were cultured on coverslips. After fixation with PBS containing 4% paraformaldehyde (Sigma-Aldrich), coverslips were incubated with rabbit anti-NeuN (1:500, Abcam) overnight. Coverslips were then washed and incubated with anti-rabbit secondary antibody conjugated with Cy3 (1:1000, Jackson ImmunoResearch Laboratories). Quantification of cell count was performed with Image J software by an investigator who

was blinded to the experimental design (National Institutes of Health). The stroke core was identified as the region in which the majority of DAPI stained nuclei were shrunken. The stroke penumbra was defined as the region of generally morphologically normal cells, approximately 450-500 μm from the boundary of the ischemic core.

Flow Cytometric Analysis

Single cells from brain, bone marrow, blood and spleen were prepared for flow cytometric analysis (FACS) at 6h, 12h, 1d, 2d, 3d, 5d and 7d after tMCAO. Bone marrow, blood and spleen were extracted before animals were perfused with ice-cold saline. Brains were dissected, and ipsilateral hemispheres were collected after saline perfusion. Each hemisphere was subjected to 0.25% trypsin-EDTA (Thermo Fisher) digestion at 37°C for 25 minutes. Brain tissue was then pressed through a cell strainer (70 μm , Thermo Fisher). Brain cells were separated from myelin debris by centrifugation in 30%/70% Percoll solution (GE healthcare). Brain cells at the interface were collected, washed with PBS and subjected to further staining. The spleen was homogenized and pressed through a cell strainer (40 μm , Thermo Fisher). Red blood cell lysis buffer (Sigma Aldrich) was applied to get rid of red blood cells in bone marrow, spleen and blood. Bone marrow cells, spleen cells and blood leukocytes were then subjected to further staining.

Single cells from brain, spleen and blood were stained with CD45-PerCp/Cy5.5 (1:400, Biolegend), CD11b-PE (1:400, Biolegend), Ly6G-APC/Cy7 (1:400, Biolegend), F4/80-BV421 (1:400, Biolegend), CD206-Alexa Fluor 647 (1:200, BD Bioscience) and MPO-FITC (1:400, Abcam). In NLR analysis of peripheral blood, leukocytes were stained with CD45-PerCp/Cy5.5 (1:400, Biolegend), Ly6G-APC/Cy7 (1:400, Biolegend), F4/80-BV421 (1:400, Biolegend), CD3-PE (1:400, Biolegend) and B220-PE (1:400, Biolegend). In phenotypic analysis of primary culture neutrophil, cells were fixed, permeabilized and then stained with CD206-Alexa Fluor 647 (1:200, BD Bioscience) and IL10-PE (1:100, Biolegend). Flow cytometric analysis was performed using a fluorescence-activated cell sorter flow cytometer (BD Biosciences), and data was analyzed using FlowJo X 10.0.7r2 software. In experiments analyzing the engulfed and un-engulfed neutrophil by macrophages in stroke lesion, brain cells from the ipsilateral hemisphere were stained with antibody cocktail as Anti CD45-PerCP/Cy5.5, Anti CD11b-PE, Anti Ly6G-APC/Cy7 and Anti F4/80-BV421. Ly6G is a specific marker for neutrophil while F4/80 is a specific marker for macrophage. Before permeabilization, myeloid cells could rarely be co-stained with Ly6G and F4/80. After permeabilization, neutrophil engulfed by F4/80⁺ macrophage could be positively stained with Ly6G. Therefore, neutrophil was first gated with CD45^{hi}CD11b⁺Ly6G⁺, then those engulfed by macrophages was determined as F4/80⁺ (CD45^{hi}CD11b⁺Ly6G⁺F4/80⁺) cells while those un-engulfed was F4/80⁻ (CD45^{hi}CD11b⁺Ly6G⁺F4/80⁻).

Magnetic sorting of neutrophils

Single brain cells were prepared as mentioned. Four ischemic hemispheres were pooled and stained using Biotin-anti-Ly6G (Biolegend) with 1 μg antibodies per 10⁶ cells. Cells were washed with PBS and further stained with anti-Biotin microbeads (Miltenyi Biotec) for 1 μg antibodies per 10⁶ cells. After two washes with PBS, cells were subjected to positive selection program using autoMACS (Miltenyi Biotec). Cells were washed and then stained

with goat anti-CD206 (1:500, R&D system) or rabbit anti-MPO (1:500, R&D system) for 30min at room temperature. After 3 washes, cells were dropped on slides and mounted with Fluoromount-G (Southern Biotech).

Real Time Polymerase Chain Reaction (RT-PCR)

Total RNA was isolated from brains and primary cultured neutrophils using the RNeasy Mini Kit (QIAGEN) according to the manufacturer's instructions. The integrity of total RNA was evaluated using a denaturing agarose gel stained with ethidium bromide. One μg RNA (OD260nm/OD280nm = 1.8-2.2) was used to synthesize the first strand of cDNA using the Prime Script RT reagent Kit (Takara). PCR was performed on a 7500 fast (ABI) RT-PCR machine using SYBR Premix Ex Taq (Takara). The following primers were used (mouse): CCL5 F: AAGTGTGTGCCAACCAGAG, CCL5 R: CCCATTTTCCCAGGACCGAG, CXCL1 F: TGGCTGGGATTCACCTCAAG, CXCL1 R: CCGTTACTTGGGGACACCTT, CXCL2 F: CATAGCCACTCTCAAGGGCG, CXCL2 R: AGGTACGATCCAGGCTTCCC, CXCL3 F: CATCCAGAGCTTGACGGTGA, CXCL3 R: ACACATCCAGACACCGTTGG, CXCL5 F: CCCCTTCCTCAGTCATAGCC, CXCL5 R: CTTCCACCGTAGGGCACTG, CXCL7 F: CCTGGCGTCAAGAGAATCGT, CXCL7 R: CTTGGCTTGCCCGTCTTCAT, MMP1a F: ACTACAAGTACAACCCAAGAAA, MMP1a R: AGCTGGGCACAATAGGGATT, MMP2 F: AACGGTCCGGAATACAGCAG, MMP2 R: GTAAACAAGGCTTCATGGGGG, MMP3 F: CCCTGGGACTCTACCACTCA, MMP3 R: AGTCTGAGAGATTTGCGCC, MMP8 F: CCACACACAGCTTGCCAATG, MMP8 R: GCTTCTCTGCAACCATCGTG, MMP9 F: CCAGCCGACTTTTGTGGTCT, MMP9 R: TGGCCTTTAGTGTCTGGCTG, MMP10 F: ATGGACACTTGCACCCTCAG, MMP10 R: GGTGGAAGTTAGCTGGGCTT, MMP13 F: GGAGCCCTGATGTTTCCCAT, MMP13 R: ATCAAGGGATAGGGCTGGGT, TIMP1 F: GAGACACACCAGAGCAGATACC, TIMP1 R: TGGTCTCGTTGATTTCTGGGG, TIMP2 F: CAGCCTCTCCCGTCTTTTGT, TIMP2 R: GTGGCTAGAAACCCAGCAT, IFN α F: CTGGTCAACCTGCTCTCTAGG, IFN α R: ACTTAGGACAGGGATGGCTTTCT, IFN γ F: ATGAACGCTACACACTGCATC, IFN γ R: CCATCCTTTTGCCAGTTCCTC, IL-12a F: CCTTGCATCTGGCGTCTACA, IL-12a R: GTCTTCAGCAGGTTTCGGGA, IL-23 F: TGGAGCAACTTCACACCTCC, IL-23 R: GGCAGCTATGGCCAAAAGG, Lymphotoxin β F: ACGGGTCGTTATGGTACAG, Lymphotoxin β R: CCCTCTCCTGTAGTCCACCA, BAFF F: TACCGAGGTTTCAGCAACACC, BAFF R: TTCGTATAGTCGGCGTGTGCG, TLR7 F: CAAAGCACGCAGCTCAAAGG, TLR7 R: GGGAGCCAAGGACATCTTTCT, TLR9 F: TGACCATTGAGCCCAGAACC, TLR9 R: GCAGTTCCTGTCATGAAGA, PAD4 F: GGATGGTTGGGCTTCCACAG, PAD4 R: TCCAATGTGCTTTGCGGAGG, NLRP3 F: ACGAGTCCTGGTACTTTGTAT, NLRP3 R: CTTTCTCGGGCGGGTAATCTT For real time PCR, the samples were heated to 95°C for 30 seconds; followed by 40 cycles with denaturation at 95°C for 5 seconds, annealing and extension at 60°C for 34 seconds, and a final extension at 72°C for 1 minute. The expression levels of the mRNAs were then reported as fold change vs Sham brain or vehicle treated neutrophils.

Primary Neutrophil-Enriched Culture and Stimulation

Primary neutrophil enriched cultures were prepared from bone marrow of 8 to 10-week-old healthy C57BL/6J male mice using EasySep Mouse Neutrophil Enrichment Kit (Stem Cell,

Cat. N0. 19762) according to manufacturer's instructions. For polarization, neutrophils were treated with lipopolysaccharide (LPS, 1µg/ml, Sigma) and interferon γ (IFN γ , 20ng/ml, Peprotech) (in RPMI1640 + 10%FBS for 3h [8]) to induce N1 phenotype, or transforming growth factor- β (TGF- β , 10ng/ml, Peprotech) (in RPMI1640 + 10%FBS for 3h [8]) to induce N2 phenotype. For NETs induction, neutrophils were treated with phorbol 12-myristate 13-acetate (PMA, 20nmol/L) in serum-free cultured medium (RPMI1640) for 3h. Neutrophils without any stimulation were defined as N0. After stimulation, normal culture medium was re-applied to neutrophils and condition medium (CM) was collected 24h later.

Quantification of NETs

Formation of NETs was quantified as in previous study [16]. Briefly, in *in vitro* experiments, NETs were identified with Sytox Green staining. Sytox Green (Invitrogen, 1:30000 diluted in Hanks' Balanced Salt Solution, HBSS) was applied to neutrophils cultured on coverslips for 15min and washed with HBSS. In *in vivo* analysis of NETs formation, brain slices were collected and stained with rabbit anti-CitH3 (1:500, Abcam). Images were collected with a microscopy (Nikon). The recorded images were loaded onto Image J (NIH) for further analysis, at which time NETs were manually quantified by 2 blinded observers. Decondensed nuclei (stained with DAPI), which also positively stained with Sytox Green or CitH3 and displayed cloud-like morphology, were considered NETs and digitally recorded to prevent multiple counts. The percentages of NETs were calculated as the average of at least 4 fields, normalized to the total numbers of cells.

Primary Macrophage-Enriched Culture

Primary monocytes were prepared from bone marrow of 8 to 10-week-old healthy C57BL/6J male mice using EasySep Mouse Monocyte Isolation Kit (Stem Cell, Cat. N0. 19861) according to manufacturer's instructions. Macrophages were induced with macrophage colony stimulating factor (M-CSF) for 7 days (50ng/ml) in culture medium (RPMI1640 + 10% FBS). As for phagocytic analysis, macrophages were first labeled with CMTPX (Invitrogen) following the manufacturer's instructions. Neutrophils were first exposed to ultra violet rays for 2h and then incubated with macrophages (neutrophils : macrophages = 10 : 1) for 1h. After 2 washes with PBS, macrophages were fixed, permeabilized and neutrophils were stained with rat anti-Ly6G (1:500, BD bioscience). Macrophage phagocytic ability was calculated as neutrophils per macrophage.

Primary cortical neuronal cultures and OGD

Primary cortical neuronal cultures were prepared from E16-18 embryos of C57BL/6 mice as previously described [15]. Neuronal ischemia was induced with oxygen glucose deprivation (OGD). Briefly, culture medium (Neural basal + B27 + 2% glutamate) was retreated and was replaced by EBSS (Gibco). Neurons were then incubated in 95% N2 + 5% CO2 for 6h. After OGD, normal neuron medium was re-applied for reperfusion and condition medium (CM) was collected 24h later. To investigate the impact of neutrophil polarity to ischemic neurons, neurons were treated with various phenotypes of neutrophils (neutrophils : neurons = 1 : 4) or neutrophil CM (neutrophil CM : neuron medium = 1 : 1) right after OGD for 24h. Neuronal viability was assessed with NeuN staining.

Scanning electronic microscopy (SEM)

Mice were sacrificed at 2d after tMCAO. Mice were first perfused with 2.5% glutaraldehyde (Sigma). Brain tissues within the infarct ($\sim 1.0\text{mm}^3$) were collected and subjected to SEM.

Statistic Analysis

Results in the current study were presented as mean \pm standard error of the mean. The differences in the means among multiple groups were analyzed using one- or two-way analysis of variance (ANOVA). When ANOVA showed significant differences, pair-wise comparisons between means were tested by Dunnett tests. The Student's t-test was used for two-group comparisons. In all analyses, $P < 0.05$ was considered statistically significant. To assess correlation between neutrophils in the peripheral blood and stroke outcomes, linear regression analysis was performed. $P < 0.05$ was considered statistically significant in linear regression and R^2 was recorded.

Results

Early elevation of neutrophils in peripheral blood indicates detrimental outcomes of ischemic stroke

A total of 225 patients with acute ischemic stroke diagnosed within 24 hours of symptom onset and 56 age and gender matched healthy controls were included in the study. Among them, infection was evident in 58 AIS patients. Patient demographics including comorbidities were summarized in Table S1 and patient inclusion process was displayed in Fig. S1. Compared with healthy controls, the numbers of neutrophils and neutrophil to lymphocyte ratio (NLR) in peripheral blood increased soon after stroke onset in patients with or without infection (Fig. 1a), among which 30 patients with infection showed neutrophilic granulocytosis (neutrophil count $> 7.5 \times 10^9/\text{L}$). In AIS patients with infections, both neutrophil counts and NLR showed no significant correlation with NIHSS scores or infarct diameters (Data not shown). In AIS patients without infection, NLR, but not neutrophil counts, was positively correlated with higher NIHSS scores (Fig. 1b, $R^2 = 0.07$, $P = 0.0006$). To analyze the correlation of peripheral neutrophil elevation with infarct sizes, AIS patients without infection were divided into two groups: infarction $\leq 1.5\text{cm}$ and $> 1.5\text{cm}$. In patients with infarction $\leq 1.5\text{cm}$ [9-11], the numbers of neutrophil or NLR did not show significant correlation with infarct sizes (Fig. 1c). Nevertheless, in patients with infarction $> 1.5\text{cm}$ [9-11], both neutrophil counts ($R^2 = 0.07$, $P = 0.0208$) and NLR ($R^2 = 0.07$, $P = 0.0447$) positively correlated with patients' infarct sizes (Fig. 1d). These results suggest that early increase of neutrophil in peripheral blood is able to predict worse stroke outcome especially in patients with infarction $> 1.5\text{cm}$. To better exclude the impact of infection to neutrophil fluctuation and testify the correlation between neutrophil elevation and infarct sizes, male C57/BL6 mice were pretreated with Gentamycin (0.8 mg) and Streptomycin (4mg) (S.C./daily) for consecutive 3 days before tMCAO. As expected, frequency of neutrophil and NLR in peripheral blood positively correlated with infarct volumes of mice at 1d after tMCAO. Therefore, when eliminating the intervention of infection, elevation of neutrophil indicates detrimental stroke outcome at least during the acute phase of AIS in both patients and animals.

Temporal dynamics of neutrophil after ischemic stroke

Since neutrophil is associated with stroke prognosis, we further assessed the temporal dynamics of neutrophil in bone marrow, peripheral blood, spleen and stroke lesion. Male C57/BL6 wild-type (WT) mice were subjected to tMCAO. A drop of neutrophil in bone marrow was detected before 12h after tMCAO. Frequency of neutrophil in bone marrow then recovered to that of sham operated mice at 1d and steady increased until at least 7d (Fig. 2a). Accordingly, neutrophil percentages in peripheral blood elevated before 1d after stroke, followed by gradual decrease to the level of Sham operated mice at 2d and maintained at low levels until at least 7d after tMCAO (Fig. 2a). NLR in peripheral blood showed a more sensitive reflection of neutrophil alteration. Blood NLR increased soon after stroke (6h), peaked at 12h-1d then steadily declined to Sham level until 5d after tMCAO (Fig. S2a). Constitution of neutrophils in spleen elevated soon after tMCAO at 6h, peaked at 12h then steadily declined to the level of Sham operated mice at 2d after ischemic stroke (Fig. 2a).

As to check the infiltration time line of neutrophils in stroke lesion, where neutrophil exerts immune-modulatory functions, expression time courses of chemokines that facilitate neutrophil trafficking (namely CCL5, CXCL1, CXCL2, CXCL3, CXCL5, CXCL7 [5]) were assessed. We found that mRNA expression of neutrophil attracting chemokines (CCL5, CXCL1, CXCL2, CXCL3) increased rapidly after ischemic stroke, peaked at 12h and dramatically decreased to Sham level at 48h (Fig. 2b), while the expression alteration of CXCL5 and CXCL7 was not detected (data not shown). To identify neutrophil infiltration pattern in stroke lesions, flow cytometry analysis and immuno-staining experiments were performed. Notable neutrophil infiltration was first detected at 12h after tMCAO, right after the expression peak of neutrophil attracting chemokines (12h). Neutrophil infiltration was prominent at 1-2d after stroke, when the neutrophil frequency peaked in peripheral blood. Neutrophil cell counts then decreased over time. Before 7d after tMCAO, few neutrophils were present in the ischemic hemisphere (Fig. 2c). In compliance with flow cytometric analysis, data from immuno-staining experiments further confirmed the prominent accumulation of neutrophils in stroke lesion at 1-2d after cerebral ischemia (Fig. S2b).

Neutrophils regulate post-stroke neural inflammation through various inflammatory mediators, including neutrophil elastase (NE), myeloperoxidase (MPO), matrix metalloproteinase (MMP), tissue inhibitor of metalloproteinase (TIMP), interferon (IFN), interleukin (IL), toll-like receptor (TLR), nucleotide-binding oligomerization domain-like receptor (NLR) family pyrin domain-containing 3 (NLRP3), NETs related peptidylarginine deiminase type 4 (PAD4), B cell activating factor (BAFF) and lymphotoxin, etc. To evaluate expression dynamics of inflammatory mediators related to neutrophil functions, ischemic hemispheres of male WT mice at different time points after tMCAO were collected and qPCR analysis was performed. We documented that mRNA levels of NE, MPO, MMP3, TIMP1 and IL-12 elevated in ischemic brain at 1d after stroke. MMP10, NLRP3 and BAFF showed increased mRNA levels at 2d, while mRNA expression of MMP2, MMP8, MMP9, MMP13, IFN γ , IL-23, TLR7, TLR9, and PAD4 was not increased until 3d after tMCAO (Fig. 2d and Fig. S2c).

Neutrophil phenotypes and clearance dynamics after ischemic stroke

It has been previously demonstrated that polarization towards N2 of neutrophils was beneficial to stroke outcome [6]. Nevertheless, neutrophil phenotypic alteration after ischemic stroke has not been documented. In the current study, polarization dynamics of neutrophils was explored with flow cytometry. The macrophage mannose receptor, CD206, has long been regarded as a marker of M2 macrophages and N2 neutrophils [17]. We found that the percentage of CD206⁺ N2 neutrophils in the ischemic brain was relatively stable over time after ischemic stroke, which slightly increased at 7d after tMCAO (Fig. 3a and Fig. S3a). Constitution of N2 neutrophils in blood and spleen was stable over time (Fig. 3a and Fig. S3a). Overall, mean fluorescence intensity of CD206 on infiltrated neutrophils in the ischemic brain was lower than that in blood and spleen (Fig. 3a). Therefore, immunostaining of CD206 on autoMACS-sorted neutrophils was performed. Although at a relatively low level, expression of CD206 on infiltrated neutrophils in the ischemic brain was confirmed (Fig. S3b).

The protective effect of N2 neutrophils was at least partially dependent on their preferential clearance by microglia/macrophages, thus promoting neural inflammatory resolution [6]. Therefore, neutrophil clearance time courses and the correlation with N2 polarization were explored. Singlets in the ischemic hemisphere were permeabilized and labelled with antibody-cocktail (Anti CD45-PerCP/Cy5.5, Anti CD11b-PE, Anti Ly6G-APC/Cy7 and Anti F4/80-BV421). CD45^{hi}CD11b⁺Ly6G⁺F4/80⁺ cells were determined as neutrophils engulfed by microglia/macrophages while CD45^{hi}CD11b⁺Ly6G⁺F4/80⁻ cells were recognized as un-engulfed neutrophils (Fig. 3b). The process of neutrophil clearance by microglia/macrophages started as early as 12h and peaked at 2d after stroke. The phagocytic process continued over time until at least 7d after tMCAO (Fig. 3c and Fig. S3c). Immunostaining of Iba1 and Ly6G confirmed that Iba1⁺Ly6G⁺ engulfed neutrophils were mostly detected at 2-3d after tMCAO (Fig. 3d). To explore the impact of neutrophil phenotype on neutrophil clearance, mean fluorescence intensity (MFI) of CD206 on CD45^{hi}CD11b⁺Ly6G⁺F4/80⁺ cells and CD45^{hi}CD11b⁺Ly6G⁺F4/80⁻ cells was compared. Interestingly, CD45^{hi}CD11b⁺Ly6G⁺F4/80⁺ cells showed lower expression of MPO (Fig. 3f and Fig. S3d), but higher MFI of CD206 over time (Fig. 3e and Fig. S3d), although CD206 expression in neutrophil infiltrated stroke lesions was relatively stable.

Skewing neutrophil polarity towards N2 phenotype protected against ischemic stroke

To better address the impact of neutrophil polarity on ischemic stroke, we induced N1 phenotype with IFN γ (40ng/ml) + LPS (1ug/ml), and N2 phenotype with transforming growth factor beta (TGF β , 20ng/ml) *in vitro*. IFN γ + LPS induced N1 neutrophil that showed an elevated mRNA expression of N1 markers IFN γ and TNF α (Fig. S4a), while TGF β induced N2 neutrophil that had increased mRNA expression of CD206, Arginase 1 and IL-10 (Fig. S4b). As assessed with flow cytometry, expression of CD206, the commonly used N2 marker dramatically increased after TGF β treatment (Fig. S4c) as well as the functional cytokine IL-10 production (Fig. S4d). Notably, in neutrophil before (N0) or after TGF β treatment (N2), CD206⁺ cells displayed prominently higher expression of IL-10 than CD206⁻ cells (Fig. S4e).

To evaluate the impact of neutrophil polarity on survival of ischemic neuron *in vitro*, primary mouse neurons were first subjected to 6h oxygen-glucose deprivation (OGD), then were treated with neutrophil conditioned medium (CM) or co-cultured with different subsets of neutrophils (Fig. 4a). Treatment of N0 or N2 CM failed to cause further decline in neuron counts after OGD, while N1 CM exacerbated post-OGD neuronal death (Fig. 4b). In comparison, neurons co-cultured with N0 or N1 neutrophils were further lost after OGD, while co-culturing with N2 neutrophils hardly affected the viability of ischemic neurons (Fig. 4b). Previous study indicated that N2 neutrophil protected against ischemic stroke at least partially dependent on their promotion of self-clearance by microglia/macrophage [6]. To testify the impact of neutrophil polarity on macrophage phagocytic activities, we subjected neutrophils to macrophage phagocytosis assay. Indeed, N2 neutrophils facilitated macrophage phagocytosis *in vitro*, while N1 showed no impact on macrophage engulfment (Fig. S4f).

To further analyze the impact of N2 neutrophil on stroke outcome, TGF β was injected to mice at 1d before tMCAO to skew neutrophil towards N2 phenotype (Fig. 4c). As the proportion of N2 neutrophil increased (Fig. 4d), infarct volumes of mice declined (Fig. 4e), which confirmed that skewing neutrophils towards N2 phenotype was protective to cerebral ischemic stroke.

Time courses of neutrophil extracellular traps (NETs) formation after ischemic stroke

Formation of NETs is a process that combats invading microbes. Although the molecular mechanism of NETs remains to be elusive, citrullination of histone [18] and reactive oxygen species (ROS) proceeded by MPO [7] have been proven to be indispensable for NETs formation. It is not until recently that NETs were detected in aseptic lesions [8]. In the current study, we documented NETs in ischemic lesions by co-labelling citrullinated histone H3 (CitH3) and Ly6G (Fig. 5a). We found that NETs formation peaked at 2-3d after ischemic stroke within the stroke lesion in both the striatum and cortex (Fig. 5b). In consistence, NETs formation was detected with immunol staining of chromatin dye Sytox green (green) and neutrophil elastase (NE, red) in stroke lesion with fluorescence microscopy (Fig. 5c) and with SEM (Fig. 5d) at 2d after tMCAO. Since MPO plays a critical role in NETs formation, expression dynamics of MPO in neutrophils was assessed with flow cytometry. In neutrophils infiltrated into the ipsilateral brain, MPO MFI was highest at 1d after tMCAO, right before the peak of NETs formation (Fig. 5d and Fig. S5). In peripheral blood, MPO expression in neutrophils was down-regulated at 12h-1d after tMCAO and rapidly recovered to the level before stroke (Fig. 5d and Fig. S5). Surprisingly, MPO MFI of neutrophils in spleen maintained stable over time (Fig. 5d and Fig. S5). The presence of NETs in stroke lesion might exert detrimental impact on the already vulnerable neural tissues. In *in vitro* experiments, we found that applying CM of NETs forming neutrophils to ischemic neuron, or co-culturing NETs forming neutrophils with ischemic neuron could both exacerbate post-OGD neuronal death (Fig. 4b), although NETs formation did not affect neutrophil clearance by macrophage (Fig. S4f). Therefore, preventing NETs formation could be a promising therapeutic strategy in ischemic stroke.

Neuronal ischemia directed neutrophil away from N2 phenotype and exacerbated NETs formation

Our results showed that N0 CM had almost no impact on neuronal viability, while co-culturing ischemic neurons with N0 cell significantly aggravated neuronal death after OGD, indicating that ischemic neurons manipulated neutrophil functions. To assess the impact of ischemic neurons to neutrophils, OGD conditioned medium (OGD CM) of neurons was used to treat neutrophils (Fig. 6a) and neutrophil polarization and NETs formation were assessed. As analyzed with flow cytometry, neuron OGD CM decreased CD206 protein expression in neutrophils (Fig. 6b). Meanwhile, mRNA levels of CD206, Arginase 1 (Arg1), IL-10 and TGF β were decreased after neuron OGD CM treatment (Fig. 6c). Since NETs had a destructive impact on ischemic neurons and had been detected in the ischemic lesion, we again evaluated whether neuron OGD CM promoted NETs formation. As expected, the presence of NETs detected with Sytox green increased after neuron OGD CM treatment (Fig. 6e) although MPO expression was not affected (Fig. 6d). In conclusion, ischemic neurons drove neutrophil polarization away from the beneficial N2 phenotype and promoted NETs formation.

Discussion

It has been widely recognized that neuroinflammation promotes secondary tissue damage in the ischemic brain [19-24]. Neutrophils are among the first immune cells to infiltrate into brain lesions after ischemic stroke. Timely infiltration of neutrophils is followed by rapid responses within stroke lesions. The present study described and summarized time course of neutrophil attracting chemokine expression, neutrophil infiltration, neutrophil related inflammatory alteration, neutrophil polarization and NETs formation. Interaction between neutrophils and macrophages or ischemic neurons were also explored.

Neutrophils in peripheral blood from stroke patients elevated within the first 24h after symptom onset. Our results suggested that the elevation of neutrophils was positively correlated with stroke outcomes including NIHSS scores and infarct sizes in patients with infarction > 1.5cm and when infection was excluded, which indicates that early increase of neutrophils in peripheral blood was able to predict worse stroke outcome especially in patients with infarction > 1.5cm. However, since the NIHSS scores is not sensitive to the lesion sizes, the correlation of neutrophil elevation with NIHSS scores and that with infarct sizes was not totally consistent. To better exclude the impact of infections on neutrophil frequency after stroke, mice were pre-treated with antibiotics before cerebral ischemia. Correlation of neutrophil counts and infarct sizes was consistent in mice and patients. Since systemic reviews and studies of meta-analysis indicated that preventive antibiotics treatments have little impact on stroke outcome although incidence of infections might be reduced, we believe that the off-target effects of the antibiotics on stroke outcomes could be neglected. In the current study, part of the included AIS patients had co-morbidities while the interfering factors in mice could be neglected. This explained why the correlation of neutrophil frequency with stroke outcomes in mice was high while that in patients was relatively low. Nevertheless, co-morbidities in AIS patients without infection were mostly chronic diseases. Therefore, the co-morbidities might not have a great impact on the

constitution of neutrophil in patients' peripheral blood. Thus, the data from ischemic stroke models in mice could at least partially reflect the situation in patients.

Increased neutrophil counts in the peripheral blood after the onset of ischemic stroke revealed an acute response by the immune system. From the peripheral blood, neutrophils infiltrate into the stroke lesion and participate in the post-stroke neural inflammation. It has documented that neutrophils arrived soon after permanent MCAO and dominant in perivascular areas including leptomeninges (6h), cortical basal lamina and cortical Virchow-Robin (15h) in mice brains as assessed with confocal microscopy [25]. It was not until 24h that neutrophils were detected in the brain parenchyma [25]. In the current study, we first comprehensively perfused mice with saline then evaluated neutrophil infiltration in the brain parenchyma with flow cytometry. We found that notable neutrophil infiltration was first detected at 12h and the infiltration into the parenchyma peaked at 1-2d after transient MCAO, which was in line with the previous study [25].

Infiltrated neutrophils exerted elaborate functions in stroke lesion. Depletion of neutrophils led to decreased infarct volume in stroke mice [6], which altogether indicated that neutrophils played a relative detrimental role in stroke lesions, at least during the acute phase of ischemic stroke. However, neutrophils are the key defense to infection. Thus, decreasing neutrophil population after stroke is not applicable. Since neutrophils exert elaborate functions in the ischemic brain, regulating and controlling neutrophil behavior in stroke lesions could be a therapeutic strategy.

Neutrophils display functional diversity in the ischemic brain. Similar to macrophages, neutrophils show phenotypic plasticity. N1 is the pro-inflammatory subset for secreting various harmful inflammatory mediators such as IFN γ and TNF α [26], while the N2 phenotype was shown to be protective in ischemic stroke [6]. In the current study, we found that CD206 expression of neutrophil in stroke lesion had been at an disadvantage until 7d after tMCAO. In myocardial infarction, which caused aseptic inflammation as in cerebral ischemic stroke, the dynamics of N2 neutrophil showed similar time line with the finding in our experiments. The percentage of CD206⁺ neutrophil increased over time (from 2.4 \pm 0.6% at Day 1 to 18.1 \pm 3.0% at Day 7) post myocardial infarction [27]. On the other hand, we found that the macrophage engulfed neutrophil expressed a significantly higher level of CD206 compared to those un-engulfed, which could be a result from stronger phagocytic function of CD206⁺ macrophages or promotion of phagocytosis by CD206⁺ neutrophils. On the other hand, *in vitro* data confirmed that N2 neutrophils facilitated clearance by macrophages. These results indicate that N2 phenotype promotes self-clearance of neutrophils, which accelerates withdrawal of neutrophils and benefits inflammatory resolution after stroke. Our *in vivo* data demonstrated that when screwing neutrophil polarization towards N2 phenotype with TGF β pretreatment, stroke outcomes of mice significantly improved. TGF β has efficient anti-inflammatory functions. The effects of reduced disease severity of stroke after TGF β pretreatment may not be solely attributed to increased N2 population. Even so, since TGF β was systemically pretreated and stroke outcomes were evaluated at early time point (1d) in the study when other immune cells beside neutrophil were still in periphery, the protective effect of systemic TGF β treatment could be largely attributed to N2 polarization of neutrophil. Nevertheless, we argued that

solo N2 markers, such as CD206, may not be efficient enough to represent the neuro-protective N2 phenotype. Co-staining neutrophils with multiple N2 markers, including Arg1 and Ym1/2, could be more helpful to distinguish the beneficial cell population.

As for interaction of neutrophils and neurons, our *in vitro* data showed that different subsets of neutrophils had differential impact on neuronal viability after OGD. We found that co-culturing neurons with N2 neutrophil cells did no harm to neuronal viability, while N1 or N0 cells exacerbated neuronal death after OGD. Although N2 neutrophils failed to enhance viability of ischemic neurons, the phenotype was less detrimental to the injured neurons. However, neuronal ischemia was prone to drive neutrophils away from the N2 phenotype. Considering the benefit to inflammatory resolution of the N2 population, re-polarizing neutrophil towards N2 phenotype could be a promising therapeutic strategy for ischemic stroke.

Extracellular trap formation is one of the functional characteristics of neutrophils. NETs formation was most detected and studied in infectious diseases and was recently found to be involved in aseptic inflammation [8]. It has been documented that the presence of NETs was a predictor of worse outcomes in myocardial infarction [28] and inhibiting NETs formation could efficiently protect against myocardial ischemia [29]. Therefore, formation of NETs might play a detrimental role in aseptic inflammation including ischemic stroke. Nevertheless, understanding of NETs in cerebral ischemia remained to be elusive. The current study showed for the first time that NETs were present in stroke lesions. The function of MPO is indispensable in NETs formation [30]. We illustrated that MPO expression in infiltrated neutrophils peaked at 1d after stroke, before the NETs forming peak were detected (2-3d), which is in accordance with the processing order of NETs formation. Our *in vitro* data demonstrated that neuronal ischemia promoted NETs formation, and NETs further increased neuronal death after ischemic injury. Therefore, the adverse impact of NETs to ischemic neuronal tissue is concerning. To inhibit NETs formation, or to enhanced NETs resolution in stroke lesions could be therapeutic target for ischemic stroke and are both worth studying in more depth.

In conclusion, we found that neutrophils are summoned by chemokines and exert elaborated functions in ischemic lesions. Directing neutrophil towards N2 phenotype protected against ischemic stroke while N1 and NETs formation aggravated damage of ischemic neurons. Nevertheless, the molecular mechanism of N2 neutrophil interaction with macrophages needs further exploration. NETs formation was first identified in stroke lesions in this study. Nevertheless, how NETs were produced and resolved still remains indescribable. Promoting neutrophil polarization towards N2 phenotype, inhibiting NETs formation or promoting NETs resolution could be promising therapeutic targets which reduced neuronal damage after stroke.

Supplementary Material

Refer to Web version on PubMed Central for supplementary material.

Acknowledgments

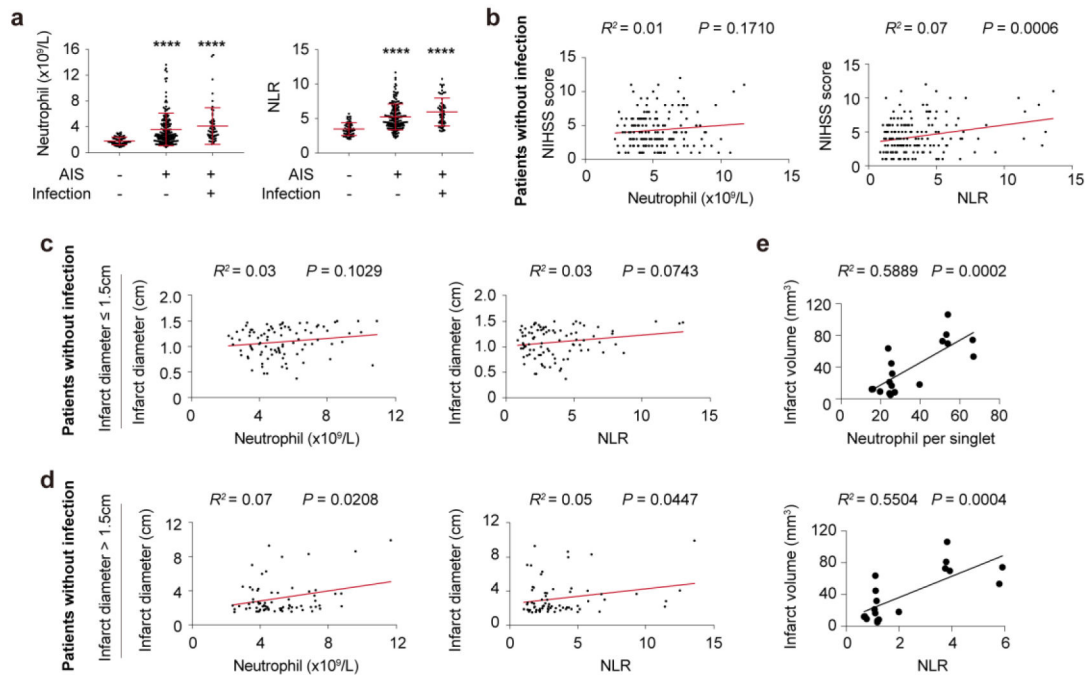
Funding

This work was supported by the Chinese Natural Science Foundation (NCSF) grants (81671178 to Z. L.). Z. L. is also supported by the Guangdong Natural Science Foundation grant (2017A030311013).

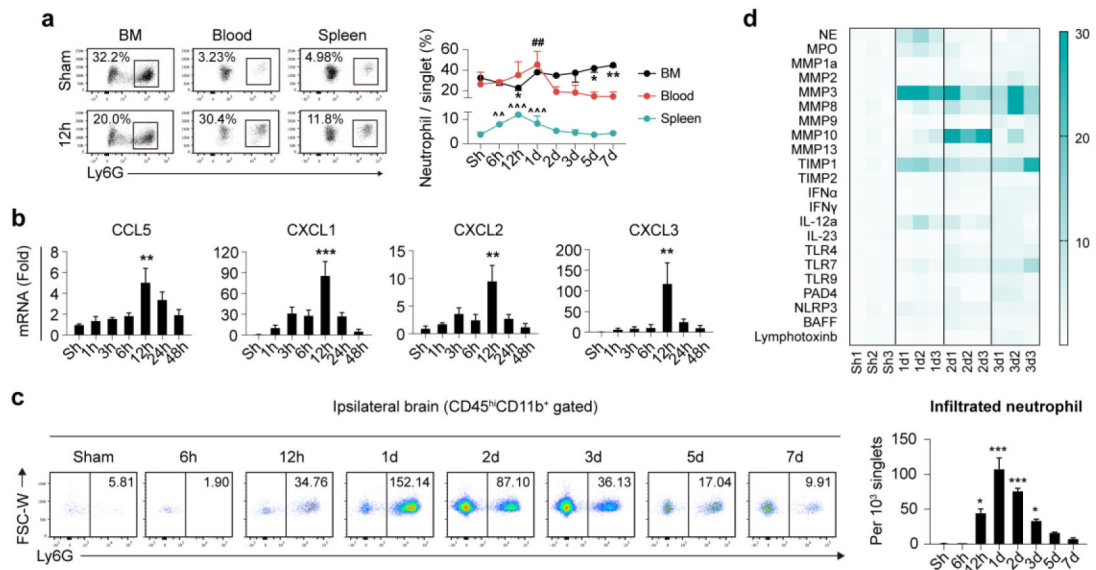
References:

1. Dirnagl U, Iadecola C, Moskowitz MA. Pathobiology of ischaemic stroke: an integrated view. *TRENDS NEUROSCI.* 1999;22:391–397 [PubMed: 10441299]
2. Shimamura N, Katagai T, Kakuta K, et al. Rehabilitation and the Neural Network After Stroke. *Transl Stroke Res.* 2017;8:507–514 [PubMed: 28681346]
3. Gelderblom M, Leyboldt F, Steinbach K, et al. Temporal and spatial dynamics of cerebral immune cell accumulation in stroke. *STROKE.* 2009;40:1849–1857 [PubMed: 19265055]
4. Wu L, Walas S, Leung W, et al. Neuregulin1-beta decreases IL-1beta-induced neutrophil adhesion to human brain microvascular endothelial cells. *Transl Stroke Res.* 2015;6:116–124 [PubMed: 24863743]
5. Griffith JW, Sokol CL, Luster AD. Chemokines and chemokine receptors: positioning cells for host defense and immunity. *ANNU REV IMMUNOL.* 2014;32:659–702 [PubMed: 24655300]
6. Cuartero MI, Ballesteros I, Moraga A, et al. N2 neutrophils, novel players in brain inflammation after stroke: modulation by the PPARgamma agonist rosiglitazone. *STROKE.* 2013;44:3498–3508 [PubMed: 24135932]
7. Brinkmann V Neutrophil Extracellular Traps in the Second Decade. *J INNATE IMMUN.* 2018:1–8
8. Lood C, Blanco LP, Purmalek MM, et al. Neutrophil extracellular traps enriched in oxidized mitochondrial DNA are interferogenic and contribute to lupus-like disease. *NAT MED.* 2016;22:146–153 [PubMed: 26779811]
9. Jackson C, Sudlow C. Comparing risks of death and recurrent vascular events between lacunar and non-lacunar infarction. *BRAIN.* 2005;128:2507–2517 [PubMed: 16195245]
10. Traylor M, Rutten-Jacobs LC, Thijs V, et al. Genetic Associations With White Matter Hyperintensities Confer Risk of Lacunar Stroke. *STROKE.* 2016;47:1174–1179 [PubMed: 27073246]
11. Norrving B Long-term prognosis after lacunar infarction. *LANCET NEUROL.* 2003;2:238–245 [PubMed: 12849212]
12. Lee CF, Venketasubramanian N, Wong KS, Chen CL. Comparison Between the Original and Shortened Versions of the National Institutes of Health Stroke Scale in Ischemic Stroke Patients of Intermediate Severity. *STROKE.* 2016;47:236–239 [PubMed: 26628386]
13. Sucharew H, Khoury J, Moomaw CJ, et al. Profiles of the National Institutes of Health Stroke Scale items as a predictor of patient outcome. *STROKE.* 2013;44:2182–2187 [PubMed: 23704102]
14. Fiebach JB, Stief JD, Ganeshan R, et al. Reliability of Two Diameters Method in Determining Acute Infarct Size. Validation as New Imaging Biomarker. *PLOS ONE.* 2015;10:e140065
15. Stetler RA, Cao G, Gao Y, et al. Hsp27 protects against ischemic brain injury via attenuation of a novel stress-response cascade upstream of mitochondrial cell death signaling. *J NEUROSCI.* 2008;28:13038–13055 [PubMed: 19052195]
16. Knight JS, Zhao W, Luo W, et al. Peptidylarginine deiminase inhibition is immunomodulatory and vasculoprotective in murine lupus. *J CLIN INVEST.* 2013;123:2981–2993 [PubMed: 23722903]
17. Zhang X, Huang F, Li W, et al. Human Gingiva-Derived Mesenchymal Stem Cells Modulate Monocytes/Macrophages and Alleviate Atherosclerosis. *FRONT IMMUNOL.* 2018;9:878 [PubMed: 29760701]
18. Wang Y, Li M, Stadler S, et al. Histone hypercitullination mediates chromatin decondensation and neutrophil extracellular trap formation. *J CELL BIOL.* 2009;184:205–213 [PubMed: 19153223]
19. Garcia-Bonilla L, Benakis C, Moore J, Iadecola C, Anrather J. Immune mechanisms in cerebral ischemic tolerance. *Front Neurosci.* 2014;8:44 [PubMed: 24624056]

20. Zhao H, Garton T, Keep RF, Hua Y, Xi G. Microglia/Macrophage Polarization After Experimental Intracerebral Hemorrhage. *Transl Stroke Res.* 2015;6:407–409 [PubMed: 26446073]
21. Wang J, Ye Q, Xu J, et al. DRalpha1-MOG-35–55 Reduces Permanent Ischemic Brain Injury. *Transl Stroke Res.* 2017;8:284–293 [PubMed: 27988839]
22. Fan X, Jiang Y, Yu Z, et al. Annexin A2 Plus Low-Dose Tissue Plasminogen Activator Combination Attenuates Cerebrovascular Dysfunction After Focal Embolic Stroke of Rats. *Transl Stroke Res.* 2017;8:549–559 [PubMed: 28580536]
23. Li L, Tao Y, Tang J, et al. A Cannabinoid Receptor 2 Agonist Prevents Thrombin-Induced Blood-Brain Barrier Damage via the Inhibition of Microglial Activation and Matrix Metalloproteinase Expression in Rats. *Transl Stroke Res.* 2015;6:467–477 [PubMed: 26376816]
24. Yu IC, Kuo PC, Yen JH, et al. A Combination of Three Repurposed Drugs Administered at Reperfusion as a Promising Therapy for Postischemic Brain Injury. *Transl Stroke Res.* 2017;8:560–577 [PubMed: 28624878]
25. Perez-de-Puig I, Miro-Mur F, Ferrer-Ferrer M, et al. Neutrophil recruitment to the brain in mouse and human ischemic stroke. *ACTA NEUROPATHOL.* 2015;129:239–257 [PubMed: 25548073]
26. Andzinski L, Kasnitz N, Stahnke S, et al. Type I IFNs induce anti-tumor polarization of tumor associated neutrophils in mice and human. *INT J CANCER.* 2016;138:1982–1993 [PubMed: 26619320]
27. Ma Y, Yabluchanskiy A, Iyer RP, et al. Temporal neutrophil polarization following myocardial infarction. *CARDIOVASC RES.* 2016;110:51–61 [PubMed: 26825554]
28. Mangold A, Alias S, Scherz T, et al. Coronary neutrophil extracellular trap burden and deoxyribonuclease activity in ST-elevation acute coronary syndrome are predictors of ST-segment resolution and infarct size. *CIRC RES.* 2015;116:1182–1192 [PubMed: 25547404]
29. Vajen T, Koenen RR, Werner I, et al. Blocking CCL5-CXCL4 heteromerization preserves heart function after myocardial infarction by attenuating leukocyte recruitment and NETosis. *Sci Rep.* 2018;8:10647 [PubMed: 30006564]
30. Bjornsdottir H, Welin A, Michaelsson E, et al. Neutrophil NET formation is regulated from the inside by myeloperoxidase-processed reactive oxygen species. *Free Radic Biol Med.* 2015;89:1024–1035 [PubMed: 26459032]

**Fig. 1.**

Early elevation of neutrophil was correlated with detrimental outcomes of cerebral ischemic stroke. A total of 225 patients and 56 age- and gender-matched healthy controls (HC) were included in the study. **a** Comparison of neutrophil count and neutrophil to lymphocyte ratio (NLR) of AIS patients with or without infection and healthy controls (HC). **** $P < 0.0001$ compared with HC. **b** Linear regression analysis of neutrophil count or NLR with NIHSS scores at admission in AIS patients without infection ($N = 167$). **c-d** Correlation of neutrophil count or NLR with infarct diameter in patients without infection. Included AIS patients without infection were further divided into small infarction group (Infarct diameter ≤ 1.5 cm, $N = 93$) **c** and large infarction group (Infarct diameter > 1.5 cm, $N = 74$) **d**, linear regression analysis of infarct size and neutrophil of the two groups was performed respectively. **e** Linear regression analysis of neutrophil count or NLR with infarct volume of mice at 1d after tMCAO ($N = 18$).

**Fig. 2.**

Temporal and spatial dynamics of neutrophil after ischemic stroke. Male C57/BL6 mice were subjected to 60min tMCAO and sacrificed at various time points. **a** Neutrophil constitution in bone marrow (BM) blood and spleen of mice as assessed with flow cytometry. $N = 3-5$. * $P < 0.05$, ** $P < 0.01$, versus Sham in BM. ## $P < 0.01$, versus Sham in blood. ^^ $P < 0.01$, ^^ $P < 0.001$, versus Sham in spleen. **b** Expression dynamics of neutrophil attracting chemokines (mRNA level) after ischemic stroke. $N = 3$. ** $P < 0.01$, *** $P < 0.001$, versus Sham (Sh). **c** Temporal dynamics of infiltrated neutrophil after ischemic stroke as assessed with flow cytometry. Number in the representative flow panel = neutrophil per 10³ singlets in ischemic hemisphere. $N = 3-5$. * $P < 0.05$, *** $P < 0.001$, versus Sham (Sh). **d** Heat map showing expression dynamics of neutrophil related inflammatory mediators in ischemic hemisphere as analyzed with qPCR. $N = 3$. Statistic analysis was displayed in Fig. S2c. FSC, forward scatter; W, width; hi, high; NE, neutrophil elastase; MPO, myeloperoxidase; MMP, matrix metalloproteinase; TIMP, tissue inhibitor of metalloproteinase; IFN, interferon; IL, interleukin; TLR, toll-like receptor; NLRP3, nucleotide-binding oligomerization domain-like receptor (NLR) family pyrin domain-containing 3; PAD, peptidylarginine deiminase type; BAFF, B cell activating factor.

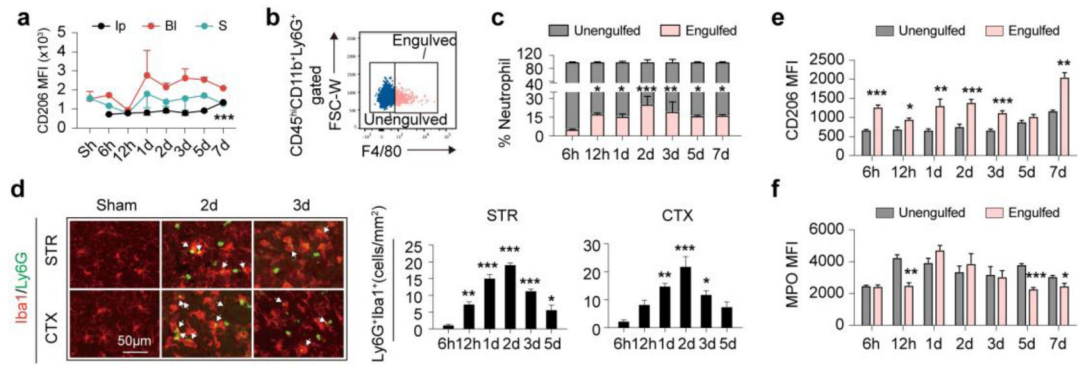
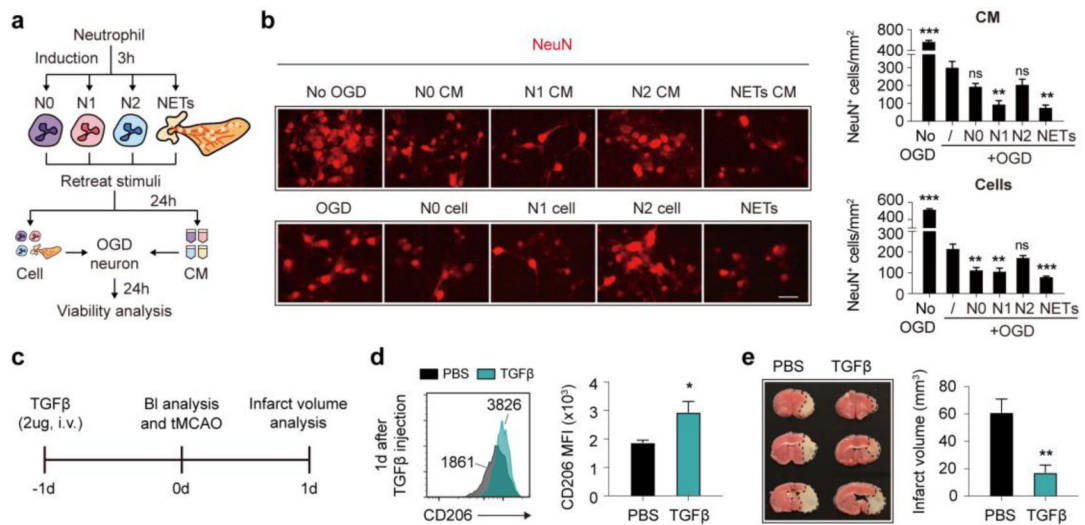
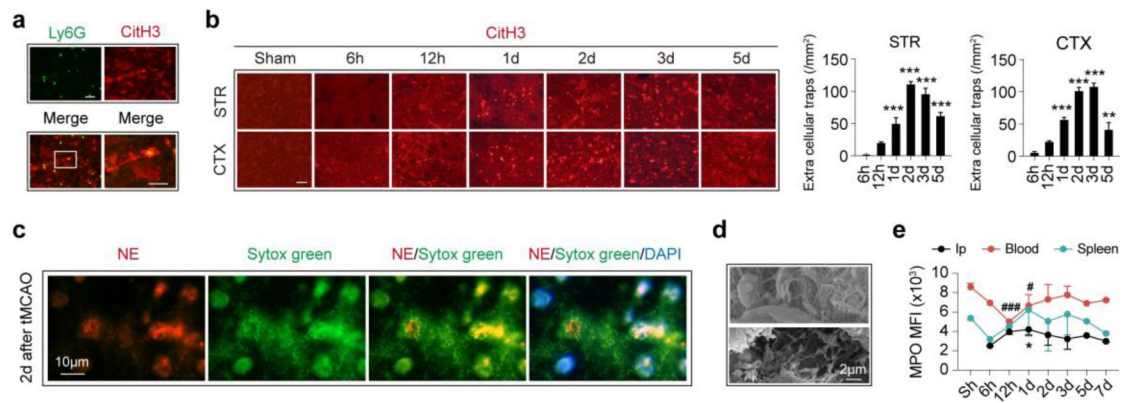


Fig. 3.

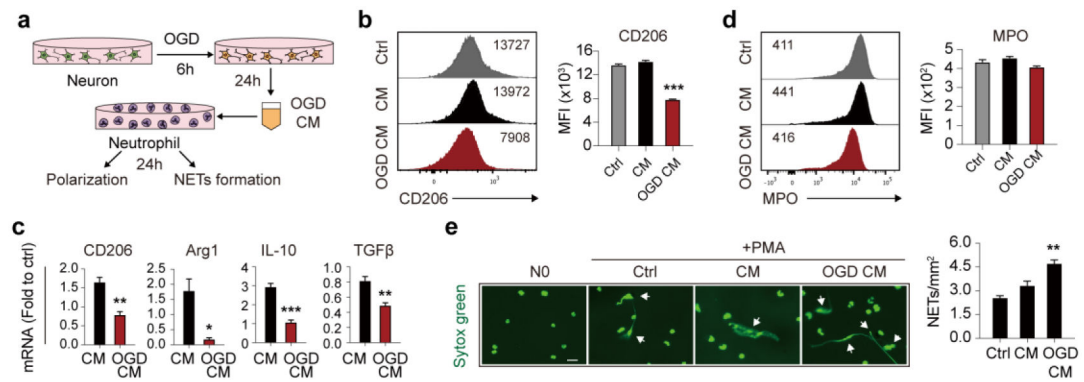
Polarization and clearance dynamics of neutrophil after ischemic stroke. **a** Polarization dynamics of neutrophils were assessed by CD206 expression with flow cytometry. Mean fluorescent intensity (MFI) of CD206 on neutrophils in Ipsilateral brain (Ip), blood (BI) and spleen (S) was analyzed. $N = 3-5$. $*** P < 0.001$, versus Sham in Ip brain. **b** Gating strategy of engulfed neutrophil ($CD45^{hi}CD11b^{+}Ly6G^{+}F4/80^{+}$) and un-engulfed neutrophils by macrophage ($CD45^{hi}CD11b^{+}Ly6G^{+}F4/80^{-}$). **c** Flow cytometry analysis of neutrophil clearance by macrophage at indicated time points. $N = 3-5$. **d** Immuno-staining of macrophages/microglia (Iba1⁺, red) phagocytosis of neutrophils (Ly6G⁺, green) in stroke lesions at indicated time points. White arrows show neutrophil engulfed by microglia/macrophage. $N = 3-4$. **e-f** Comparison of CD206 and MPO expression in engulfed and un-engulfed neutrophils by macrophages in ipsilateral brain as analyzed with flow cytometry. $N = 3-5$. $*P < 0.05$. $**P < 0.01$, $***P < 0.001$, compared with 6h.

**Fig. 4.**

Protection of N2 neutrophil against ischemic stroke. Neutrophils were isolated from bone marrow of male C57/BL6 mice with magnetic sorting. **a** Time line of neutrophil induction and treatment to ischemic neuron. **b** Viability of ischemic neuron was assessed with immuno-staining of anti-NeuN antibodies (red). Data were summarized from 3 independent experiments. ** $P < 0.01$, *** $P < 0.001$ versus OGD neuron without treatment. Scale bar = 20 μ m. **c** Time line of *in vivo* N2 induction with TGF β treatment, tMCAO and blood (BI) analysis. **d** Flow cytometric analysis of neutrophil phenotypic shift at 1d after TGF β injection (before tMCAO). $N = 9$ in each group. * $P < 0.05$, versus PBS treated group. **e** Infarct volume analysis at 1d after tMCAO with TTC staining. Dash-line outlined the infarct area. $N = 9$ in each group. ** $P < 0.01$, versus PBS treated group. NETs, neutrophil extracellular traps; OGD, oxygen glucose deprivation; CM, conditioned medium; BI, blood; TGF β , transforming growth factor beta; d, day.

**Fig. 5.**

Neutrophil extracellular traps (NETs) formation time course after ischemic stroke. NETs formation was analyzed with immuno-staining of citrullinated histone 3 (CitH3) in coronal frozen brain slices at different time points after tMCAO. **a** Representative image showing NETs formation in striatum stroke lesion (co-localization of Ly6G (green) and CitH3 (red)) at 3d after ischemic stroke. **b** NETs formation dynamics in stroke lesion at striatum (STR) and cortex (CTX) as assessed with immuno-staining of CitH3 (red). NETs formation peaked at 2-3d after tMCAO. $N = 3-4$. $**P < 0.01$, $***P < 0.001$ versus 6h. Scale bar = 20 μ m. **c** Presence of NETs formation was confirmed with immunol staining of chromatin dye Sytox green (green) and neutrophil elastase (NE) at 2d after tMCAO. Experiments were repeated for 3 times and representative images from one of the scanning were presented. **d** Presence of NETs formation was confirmed with scanning electronic microscopy (SEM) at 2d after tMCAO. $N = 4$. **e** Expression dynamics of MPO in neutrophil in ipsilateral brain (Ip), blood and spleen. $N = 3-4$. $*P < 0.05$ versus Sham in ipsilateral brain; $\#P < 0.05$, $###P < 0.001$ versus Sham in blood. CitH3, citrullinated histone 3; STR, striatum; CTX, cortex; d, day; Ip, ipsilateral brain; MFI, mean fluorescence intensity; Sh, Sham.

**Fig. 6.**

Impact of neuronal ischemia on neutrophil polarity and NETs formation. **a** Time line of neuron conditioned medium after 6h oxygen glucose deprivation (OGD CM) collection and treatment of neutrophils. **b** Flow cytometric analysis of neutrophil polarity after neuron OGD CM treatment for 24h with CD206 expression. Data were summarized from 3 independent experiments. *** $P < 0.001$ versus control (Ctrl). **c** Polarization of neutrophils after neuron OGD CM treatment for 24h was analyzed with mRNA expression of CD206, Arg1, IL-10 or TGFβ by qPCR. Data were summarized from 3 independent experiments. * $P < 0.05$, ** $P < 0.01$, *** $P < 0.001$ versus conditioned medium of healthy neuron (CM). **d** MPO expression in neutrophils after neuron OGD CM treatment for 24h was analyzed with flow cytometry. Data were summarized from 3 independent experiments. **e** Neutrophils were treated with neuron OGD CM for 24h then subjected to PMA treatment (20nmol/L for 3h) to induce NETs formation. Neutrophils treated with neuron OGD CM were prone to form NETs. Scale bar = 20μm. Data were summarized from 3 independent experiments. ** $P < 0.01$ versus control (Ctrl). OGD, oxygen glucose deprivation; CM, conditioned medium; NETs, neutrophil extracellular traps; h, hour; MFI, mean fluorescence intensity; Ctrl, control; Arg1, arginase 1.